Nodal Sensitivity-Based Smart Inverter Control for Voltage Regulation in Distribution Feeder

Oğuzhan Ceylan, *Member, IEEE*, Sumit Paudyal, *Member, IEEE*, and Ioana Pisica, *Senior Member, IEEE*

***Abstract*—Overvoltage is one of the issues in distribution grids with high penetration of photovoltaics (PVs). Centralized or droop-based methods of active power curtailment (APC) and/or reactive power control of PVs are viable solutions to prevent overvoltage. This article proposes two distributed methods to control PV inverters, which are based on nodal sensitivities. Then, the performance of the proposed methods is compared with two commonly used control methods, i.e., a distributed method that follows IEEE-1547 but uses arbitrarily chosen droops and a centralized optimal power flow (OPF) based method. Performance is evaluated using a 730-node feeder with up to 100% penetration of inverters. Based on the case studies, the key findings are: first, local droop setting as per IEEE-1547, whether the droops are arbitrarily chosen or systematically calculated using sensitivities, can eliminate overvoltage if reactive power control and APC are coordinated, second, the proposed sensitivity-based approach yields the best voltage performance index computed based on voltage profile compared to the maximum allowed upper bound, and third, OPF-based method is desirable if communication infrastructure exists and minimum energy curtailment is sought.**

***Index Terms*—Distribution grid, optimal power flow (OPF), overvoltage, photovoltaic (PV), smart inverter, voltage control.**

NOMENCLATURE

$\boldsymbol{\alpha}$	Percentage of maximum reactive power capability.
$\boldsymbol{\beta}, \boldsymbol{\gamma}$	Slope of droop curves.
$\boldsymbol{\Delta t}$	Time interval.
$\boldsymbol{\Delta V}$	Voltage change on a node.
$\Delta \boldsymbol{V}^{\text{Rq}}$	Required voltage change.
$\frac{\boldsymbol{\delta\Theta}}{\boldsymbol{\delta P}}, \frac{\boldsymbol{\delta\Theta}}{\boldsymbol{\delta Q}}, \frac{\boldsymbol{\delta V}}{\boldsymbol{\delta P}}, \frac{\boldsymbol{\delta V}}{\boldsymbol{\delta Q}}$	Sensitivities.
$\boldsymbol{\Theta}$	Voltage angle.
$\boldsymbol{\omega}$	Window of time.
$\boldsymbol{e}$	End node of a lateral.
$\boldsymbol{E}^{\text{cur}}$	Curtailed energy.
$\boldsymbol{I}$	Nodal current injection.
$\boldsymbol{j}, \boldsymbol{k}$	Set of nodes, $\boldsymbol{j}, \boldsymbol{k} \in \{\boldsymbol{1}, \boldsymbol{2}, .., \boldsymbol{N}\}$.
$\boldsymbol{l}$	Set of laterals, $\boldsymbol{l} \in \{\boldsymbol{1}, \boldsymbol{2}, \boldsymbol{3}, .., \boldsymbol{L}\}$.
$\boldsymbol{m}, \boldsymbol{n}$	Set of nodes with PVs, $\boldsymbol{m}, \boldsymbol{n} \in \{\boldsymbol{1}, \boldsymbol{2}, \boldsymbol{3}, .., \boldsymbol{M}\}$.
$\boldsymbol{P}^{\text{cur}}$	Active power curtailment of PVs.
$\boldsymbol{P}^{\boldsymbol{L}}$	Active power of load.
$\boldsymbol{P}$	Available PV generation.
$\boldsymbol{Q}^{\boldsymbol{c}}$	Unused reactive power capability of PVs.
$\boldsymbol{Q}^{\max}$	Maximum reactive power capability of PVs.
$\boldsymbol{Q}$	Reactive power output of PVs.
$\boldsymbol{Q}^{\boldsymbol{L}}$	Reactive power of load.
$\boldsymbol{r}$	Sorted reactive power capability, $\boldsymbol{r} \in \{\boldsymbol{1}, \boldsymbol{2}, \boldsymbol{3}, .., \boldsymbol{R}\}$.
$\boldsymbol{\mathcal{S}}$	Sensitivity matrix.
$\boldsymbol{S}$	Inverter rating.
$\boldsymbol{t}$	Time index, $\boldsymbol{t} \in \{\boldsymbol{1}, \boldsymbol{2}, \boldsymbol{3}, .., \boldsymbol{T}\}$.
$\boldsymbol{V}$	Nodal voltage.
$\boldsymbol{V}^{\boldsymbol{a}}, \boldsymbol{V}^{\boldsymbol{b}}, \boldsymbol{V}^{\boldsymbol{c}}, \boldsymbol{V}^{\boldsymbol{d}}$	Voltage break points.
$\boldsymbol{V}^{\boldsymbol{L}}/\boldsymbol{V}^{\boldsymbol{U}}$	Voltage lower/upper limits for inverter operation.
$\boldsymbol{V}^{\min}/\boldsymbol{V}^{\max}$	Voltage lower/upper limits for feeder operation.
$\boldsymbol{Y}$	Y-bus matrix.

Manuscript received January 4, 2021; revised March 1, 2021; accepted March 25, 2021. This work was supported in part by the National Science Foundation under Grant ECCS-2001732. *(Corresponding author: Sumit Paudyal.)*

Oğuzhan Ceylan is with the Kadir Has University, Istanbul 34083, Turkey (e-mail: oguzhan.ceylan@khas.edu.tr).

Sumit Paudyal is with the Florida International University, Miami, FL 33199 USA (e-mail: spaudyal@fiu.edu).

Ioana Pisica Paudyal is with the Brunel University London, UB8 3PH London, U.K. (e-mail: ioana.pisica@brunel.ac.uk).

Color versions of one or more figures in this article are available at https://doi.org/10.1109/JPHOTOV.2021.3070416.

Digital Object Identifier 10.1109/JPHOTOV.2021.3070416

I. INTRODUCTION

SOLAR photovoltaic (PV) systems are the fastest growing source of renewable energy being integrated to power grids [1]. This has obvious advantages, including economic benefits and less emissions. However, high penetration of rooftop PVs raises a number of concerns to the system operators. High PV penetration causes several operational challenges to the distribution grids, including overvoltage [2] and power quality [3]. During high PV generation and low load periods, there could be reverse power flow that leads to voltage rise on the low voltage (LV) feeders [4]. Overvoltage is one of the main reasons for limiting the capacity of PV that can be connected to LV systems [5]. A utility study showed that hosting capacity of LV feeder is limited by overvoltage during an extreme condition of lowest load and maximum PV generation [6].

Conventionally, volt/var regulation on distribution grids is achieved through control of legacy grid devices, such as load tap changers and switched capacitors [7], which can now be achieved through the control of smart inverters. In future distribution grids, novel grid applications can be achieved through the coordination of smart inverters [8]. For example, smart inverters can modulate active power (Watt) and reactive power (VAr)

injections necessary for system-wide volt/var support. Reactive power support from smart inverters also helps to accommodate higher penetration of distributed PVs without need of system upgrade to some extent [9]. IEEE-1547 requires smart inverters to be capable of consuming or producing reactive power when inverters are at or above 5% of their rated active power [10]. Though active power curtailment (APC) of PVs is more effective on managing distribution grid voltage due to high R/X ratio of feeders [4], [11], the reactive power control should also be considered to reduce unnecessary energy curtailment resulting from the APC-based approach alone.

Current literature on prevention of overvoltage in distribution systems with PVs is mainly divided into centralized and distributed methods for APC and reactive power dispatch. The centralized approaches solve optimal power flow (OPF) or its variants to find the dispatch of active and/or reactive power from the PVs. The centralized approaches demand communication infrastructure, whereas local approaches are droop-based and avoid the need of communication.

Lin *et al.* [12] used a droop-based (kW/V) approach for active power ($\boldsymbol{P}$) curtailment. Ghosh *et al.* in [13] proposed a droop-based $\boldsymbol{P}$ curtailment and reactive power ($\boldsymbol{Q}$) absorption method for controlling the PV inverters. Similarly, Molina-García *et al.* proposed piecewise linear droops to control the voltage with PVs [14]. Mokhtari *et al.* in [15] used droop-based approach for APC, and empirical $\boldsymbol{Q(P)}$ rules to absorb reactive power. Gagrica *et al.* in [16] used $\boldsymbol{\delta V/\delta P}$ sensitivities for droop settings. Ku *et al.* in [17] used both $\boldsymbol{\delta V/\delta P}$ and $\boldsymbol{\delta V/\delta Q}$ sensitivities to coordinate reactive power absorption and APC of PVs. Demirok *et al.* also used $\boldsymbol{\delta V/\delta P}$ and $\boldsymbol{\delta V/\delta Q}$ sensitivities to devise two droop control functions $\boldsymbol{\cos\Phi(P)}$ and $\boldsymbol{Q(V)}$ [18]. In [19], reactive power of distributed generators are dispatched based on approximate sensitivities.

The key challenge with the aforementioned local droop-based control techniques is the lack of coordinated operation, which results in nonoptimal APC. Moreover, these droop control methods also require to compute threshold power or voltage beyond which the droop becomes effective. However, the inverter operating characteristics curves $\boldsymbol{Q(V)}$, $\boldsymbol{Q(P)}$, and $\boldsymbol{P(Q)}$, as defined in the IEEE-1547 [10], are also based on local measurements, and the droops used in the studies [12]–[18] can certainly serve as a basis for the smart inverter settings as per the IEEE-1547.

One of the solutions to address the coordination challenges of decentralized control is to implement centralized control scheme. Weckx *et al.* in [20] proposed a centralized optimization-based method that would compute piecewise linear control function $\boldsymbol{Q(P)}$ to use at local controllers for locally adjusting the reactive power. Su *et al.* proposed an OPF-based approach to find $\boldsymbol{(P, Q)}$ set points of the PV inverters in [21]. Zhao *et al.* also used OPF-based formulation with adaptive weight on objective function to ensure fair curtailment [22]. Cavraro *et al.* in [23] demonstrated the value of communication for regulating voltage with PVs by showing instances where local measurement based control approaches (like in [24]) lead to infeasibility issues. Some recent works use combination of centralized and distributed approaches. Ferreira *et al.* proposed sensitivity-based

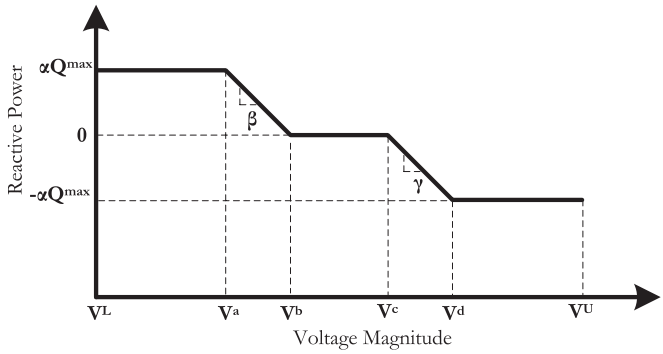

Fig. 1. An Example $\boldsymbol{Q(V)}$ curve as per IEEE-1547 [10].

($\boldsymbol{\delta V/\delta P}$) linear centralized optimization approach and a local control methods for finding optimal PV curtailment [25]. Olivier *et al.* in [26] proposed distributed control for managing reactive power and curtailing active power systematically. Though a centralized method requires communication, since the IEEE-1547 requires all smart inverters be equipped with communication capability, a centralized OPF-based approach for inverter dispatch could be feasible in future distribution grids. Moreover, the obvious advantages of centralized OPF (e.g., less APC [11], fair APC [22]) over distributed control will certainly be a reason for its adoption in future distribution grid management systems.

Since the centralized and distributed methods both for controlling PVs are gaining research attention, and both methods have advantages and shortcomings, in this work, we try to examine the performance of both approaches. In this context, the contributions of this work are as following.

1) It proposes two distributed methods to regulate voltage in PV-rich distribution networks. The first proposed method uses a sensitivity-based approach, different from the existing approaches, such as the one in [19], which includes APC in coordination with reactive power control for voltage control in distribution networks. The second proposed method combines sensitivities with the IEEE-1547 recommended piecewise droop settings.
2) Comparative analyses of the proposed methods are carried out using arbitrary droop settings of $\boldsymbol{Q(V)}$ and an OPF-based method. Monte Carlo analyses are also carried out with different PV penetration levels to examine the robustness of the proposed methods.

The rest of this article is organized as follows. Section II details the local and centralized control methods used in this work. Section III describes the MV/LV feeder used for the simulation and case studies. The main conclusions drawn from this article are provided in Section IV.

II. Local and Centralized Methods of Inverter Control

A. Reactive Power Control Rules as Per IEEE-1547

IEEE-1547 prescribes a set of droops for active and reactive power control based on local voltage at inverter node [10]. Fig. 1 shows an example $\boldsymbol{Q(V)}$ droop curve. $\boldsymbol{V^L}$ and $\boldsymbol{V^U}$ represent

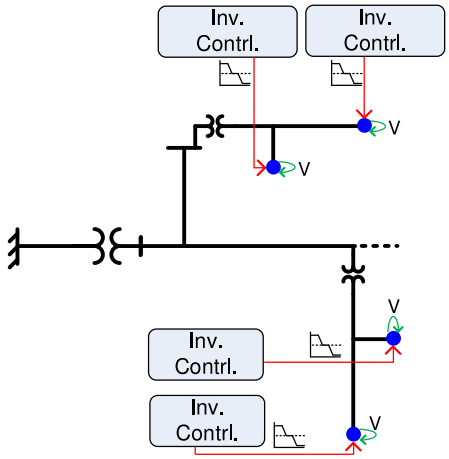

Fig. 2. Active and reactive power control based on IEEE-1547 rules.

lower and upper limits for the inverter operation, respectively. V^a, V^b, V^c, and V^d correspond to the voltage break points that define the piecewise droop settings. IEEE-1547 provides ranges for setting the break points on the $Q(V)$ and other droop curves [10]. Fig. 2 shows a schematic diagram of how control rules based on the IEEE-1547 can be implemented. It should be noted that $Q(V)$ droop settings can be dispatched on regular intervals from the control center or configured locally.

Each inverter may use different $Q(V)$ droop settings. Each inverter controller checks its local voltage magnitude and if it is smaller than V_m^a, then the inverter injects $\alpha Q_m^{\max}$, i.e., the maximum allowed reactive power injection as percentage of total reactive power capability of the inverter. If the voltage magnitude is higher than V_m^d, then the output of inverter is set to $-\alpha Q_m^{\max}$. When the measured voltage is within V_m^a and V_m^b, reactive power injection follows the slope β_m. Similarly, when the measured voltage is between V_m^b and V_m^c, then the reactive power output of the inverter follows the slope γ_m. If the measured voltage is between V_m^c and V_m^d, then the reactive power output of the inverter becomes zero. In reactive power priority mode, curtailment of active power may become necessary. To check whether APC is required or not, $P_m^2 + Q_m^2$ is compared to square of the inverter's apparent power rating S_m^2. If the latter is smaller, then active power is curtailed. The algorithm of reactive power control and APC based on the IEEE-1547 prescribed droop settings are given in Algorithm 1.

Algorithm 1: Control as Per IEEE-1547 Droops.

$$\beta_m = \frac{\alpha Q_m^{\max}}{V_m^b - V_m^a}$$

$$\gamma_m = \frac{-\alpha Q_m^{\max}}{V_m^d - V_m^c}$$

```
while t < T do
    Run Power Flow
    while m < M do
        if V_{m,t} < V_m^a then
            Q_{m,t} = α Q_m^max
        else if V_{m,t} > V_m^d then
            Q_{m,t} = −α Q_m^max
        else if V_{m,t} > V_m^a and V_{m,t} < V_m^b then
            Q_{m,t} = α Q_m^max − β_m (V_{m,t} − V_m^a)
        else
            Q_{m,t} = −α Q_m^max − γ_m (V_m^d − V_{m,t})
        end
        if Q_{m,t}^2 + P_{m,t}^2 > S_m^2 then
            P_{m,t}^cur = P_{m,t} − sqrt(S_m^2 − Q_{m,t}^2)
        end
    end
end
```

B. Proposed Approach: Power Flow Sensitivity-Based Method

A schematic of inverter control based on proposed sensitivity-based approach is shown in Fig. 3. In the proposed approach, controller works at each lateral level, and using power flow sensitivities computed offline, and based on available real-time nodal voltage measurements, active and reactive powers of PVs are dispatched in real time. The power flow sensitivity matrix can be defined as [4]

$$\mathcal{S} = \begin{bmatrix} \frac{\delta\Theta}{\delta P} & \frac{\delta\Theta}{\delta Q} \\ \frac{\delta V}{\delta P} & \frac{\delta V}{\delta Q} \end{bmatrix}. \quad (1)$$

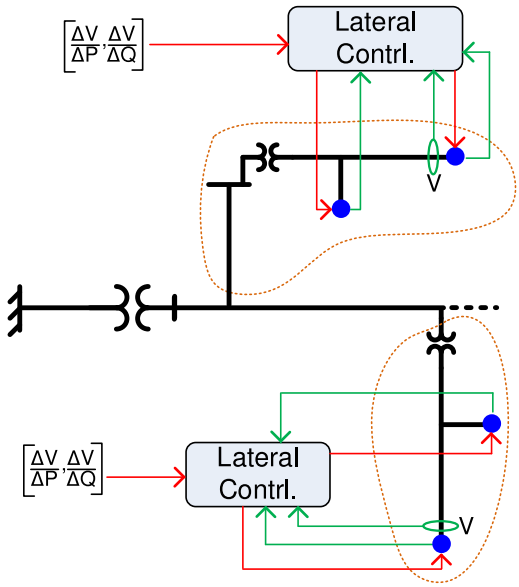

Fig. 3. Active and power control based on sensitivity-based approach.

For reactive power based voltage control, $\frac{\delta V}{\delta Q}$ are used, whereas for APC, $\frac{\delta V}{\delta P}$ are used. The coordination among multiple inverters for APC and reactive power control is achieved in the following, and further details are provided in Algorithm 2. The proposed sensitivity-based approach checks the voltage magnitudes at the end nodes of each lateral and takes the following control actions.

1) If the voltage magnitude of the end node of a lateral is within V_m^a/V_m^d, no new control action is required.
2) If the voltage magnitude of the end node of a lateral is outside V_m^a/V_m^d, all the PVs on the lateral provide active power output information to the lateral controller, which is then used to find reactive power capability of a PV using $Q_m^c = \pm\sqrt{S_m^2 - P_m^2}$. Also, the sensor on the end node of the lateral provides the voltage information, which is then used by the controller to compute voltage increment ($\Delta V_m = Q_m^c \frac{\delta V_e}{\delta Q_m}$) using the reactive power capability and sensitivity and sorted in a descending order.
3) The difference of measured voltage magnitude at the end node of a lateral and the minimum/maximum allowed limits ($V^{\min}/V^{\max}$) is calculated, i.e., ΔV_e^{Rq}. Then, the first R sorted reactive capability information that is sufficient to bring the voltage magnitude within the limits is selected, and dispatch signals are sent to the corresponding inverter controllers.
4) If the reactive power capability of the inverters are not enough in maintaining the voltage, then we apply APC based on $\frac{\delta V_e}{\delta P_m}$ to compensate the remaining voltage difference. For fairness across PVs, we propose to curtail PV active power equally from all inverters using average sensitivity values.

C. Proposed Approach: Power Flow Sensitivities-Based Droops as Per IEEE-1547

The droops $Q(V)$, as shown in Fig. 1, could be obtained systematically using the power flow sensitivities. Thus, the reactive power to voltage sensitivities obtained from (1) are used to derive the slopes of $Q(V)$ droops as following:

$$\beta_m = \gamma_m = \frac{\delta Q_m}{\delta V_m}. \tag{2}$$

The droop settings $Q(V)$ obtained are sent to the inverter controllers at regular time interval, and then the local controllers manage the reactive power output of each inverters, as shown in Fig. 4. In reactive power priority mode, curtailment of active power may become necessary as in the method in Section III-A. To check whether APC is required or not, $P_m^2 + Q_m^2$ is compared to square of the inverter's apparent power rating S_m^2. If the latter is smaller, then active power is curtailed. The algorithm of reactive power control and APC is similar to one in Algorithm 1.

D. OPF-Based Control

For the centralized approach, OPF model can be solved to minimize APC utilizing inverters' reactive power capability while maintaining operating limits and power balance equations. The control schema for an OPF-based method for voltage control is provided in Fig. 5. A generic OPF model for this purpose can be formulated as

$$\text{Min:} \quad E^{\text{cur}} = \sum_{m,t} P_{m,t}^{\text{cur}} \, \Delta t \tag{3}$$

subject to:

Algorithm 2: Sensitivity-Based Method of Control.

```
while t < T do
    Run Power Flow
    while l < L do
        sort ΔV_{m,t} = Q^c_{m,t} δV_{e,t}/δQ_{m,t}
        if V_{e,t} > V^d_e then
            ΔV^{Rq}_{e,t} = V^d_e − V_{e,t}
        end
        if V_{e,t} < V^a_e then
            ΔV^{Rq}_{e,t} = V_{e,t} − V^a_e
        end
        while r < R do
            if ΔV^{Rq}_{e,t} < 0 then
                Q_{m,t} = Q_{m,t} + Q^c_{m,t}
                ΔV^{Rq}_{e,t} = ΔV^{Rq}_{e,t} + ΔV_{m,t}
            else if ΔV^{Rq}_{e,t} > 0 then
                Q_{m,t} = Q_{m,t} − Q^c_{m,t}
                ΔV^{Rq}_{e,t} = ΔV^{Rq}_{e,t} − ΔV_{m,t}
            else
                break
            end
        end
        if ΔV^{Rq}_{e,t} > 0 then
            while m < M do
                P^{cur}_{m,t} = ΔV^{Rq}_{e,t} / ((1/M) Σ_n δV_{e,t}/δP_{n,t})
            end
        end
    end
end
```

$$I_{j,t} = \sum_{k \in N} Y_{j,k} \, V_{k,t} \quad \forall j, t \tag{4}$$

$$P_{j,t} - P_{j,t}^{\text{cur}} - P_{j,t}^{L} = \text{Real}\left(V_{j,t} \; I_{j,t}^{*}\right) \quad \forall j, t \tag{5}$$

$$Q_{j,t} - Q_{j,t}^{L} = \text{Imag}\left(V_{j,t} \; I_{j,t}^{*}\right) \quad \forall j, t \tag{6}$$

$$V^{\min} \leq |V_{m,t}| \leq V^{\max} \quad \forall m, t \tag{7}$$

$$Q_{m,t} \leq \sqrt{S_m^2 - \left(P_{m,t} - P_{m,t}^{\text{cur}}\right)^2} \quad \forall m, t \tag{8}$$

$$Q_{m,t} \geq -\sqrt{S_m^2 - \left(P_{m,t} - P_{m,t}^{\text{cur}}\right)^2} \quad \forall m, t. \tag{9}$$

In the aforementioned formulation, (3) represents energy curtailment of PVs, (4) represents current injection equations at each node, (5) represents load/PV active power model, (6) represents load/PV reactive power model, (7) represents limits on the voltage magnitude, and (8) and (9) represent lower and upper bounds on the reactive power of PVs.

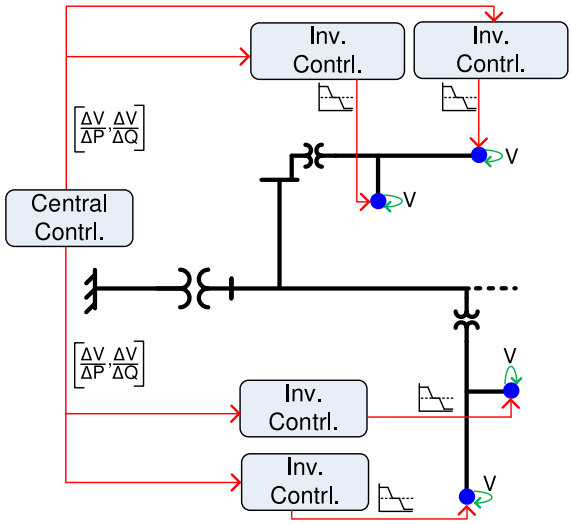

Fig. 4. Control based on droops obtained from power flow sensitivities.

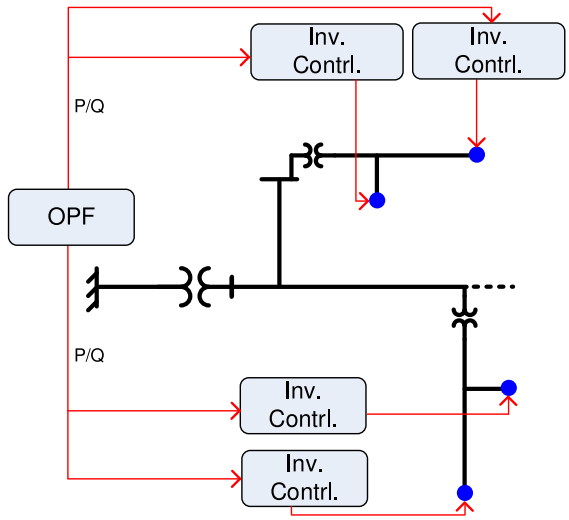

Fig. 5. Inverter control based on OPF solution.

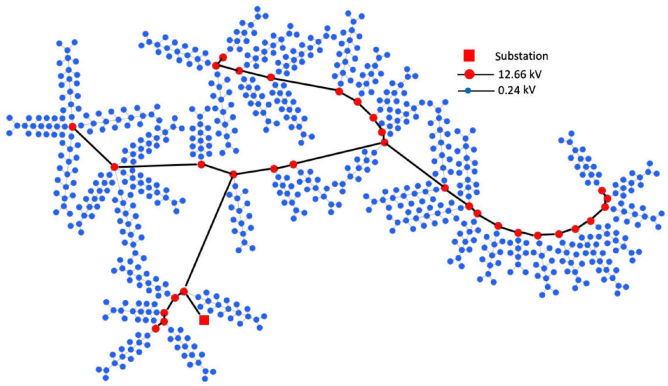

Fig. 6. 730-node MV/LV feeder used for the case studies [28].

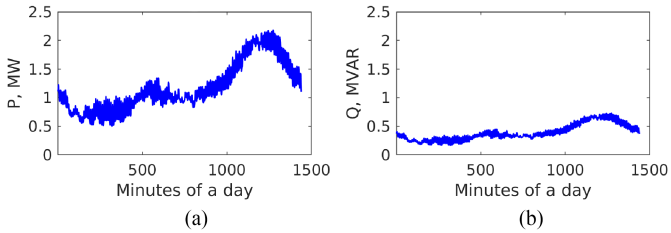

Fig. 7. Total loads. (a) Active load profile. (b) Reactive load profile.

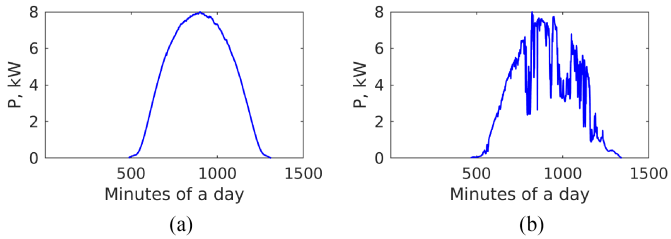

Fig. 8. PV profiles. (a) PV-1 (sunny day). (b) PV-2 (cloudy day).

III. Numerical Simulations

This section provides details of performance studies of control based on the IEEE-1547 with arbitrary slopes, sensitivity-based method, IEEE-1547 with sensitivity-based droop settings, and OPF-based method in terms of voltage profile and power/energy curtailment.

A. Test System and Setup

Baran and Wu system [27] modified to a 730-node feeder as used in [28] (see Fig. 6) was adopted for the studies with 70% and 100% PV penetration levels (by the number of LV nodes). These correspond to 306 and 436 number of inverters, respectively. Each inverter is rated 8 kW. We considered $\boldsymbol{V}^{\boldsymbol{L}}$=0.88 p.u., $\boldsymbol{V}^{\boldsymbol{U}}$=1.1 p.u., $\boldsymbol{V}^{\min}$=0.95 p.u., and $\boldsymbol{V}^{\max}$=1.05 p.u.

Load profiles are similar to that used in [11] and represents realistic data. Fig. 7 shows net active and reactive power loads with 1-min resolution for a typical day. We used two PV profiles, as shown in Fig. 8: one corresponds to a sunny day (PV-1) and the second profile corresponds to a cloudy day (PV-2). We used Newton–Raphson based method in MATLAB to perform daily load flow simulations on 1-min resolution for the distributed approaches. For OPF-based approach, we modeled using GAMS and solved using KNITRO solver.

B. IEEE-1547 With Arbitrary Droop Settings

IEEE-1547 prescribes range for the voltage break points for the $\boldsymbol{Q}(\boldsymbol{V})$ curve in Fig. 1 [10]. Thus, we created random droop settings by arbitrarily choosing $\boldsymbol{V}^{\boldsymbol{a}}$, $\boldsymbol{V}^{\boldsymbol{b}}$, $\boldsymbol{V}^{\boldsymbol{c}}$, and $\boldsymbol{V}^{\boldsymbol{d}}$ within the range prescribed in [10] for each inverter. Then, we performed a series of daily simulations with 1-min time resolution, and the voltage profiles (maximum voltage on the feeder) obtained from the base case (assuming no control over PVs) simulation with control of PVs are compared in Fig. 9. The base case shows

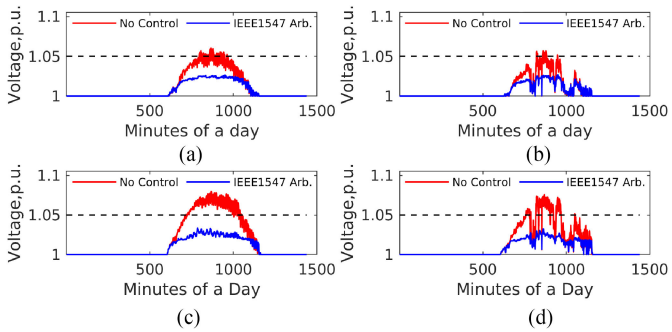

Fig. 9. Max. voltage with base case versus IEEE-1547 with arbitrary droops. (a) 70% PV, PV-1. (b) 70% PV, PV-2. (c) 100% PV, PV-1. (d) 100% PV, PV-2.

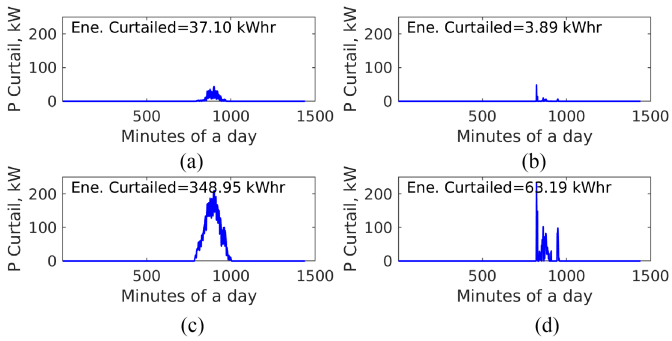

Fig. 10. APC obtained from the IEEE-1547 with arbitrary droop settings. (a) 70% PV, PV-1. (b) 70% PV, PV-2. (c) 100% PV, PV-1. (d) 100% PV, PV-2.

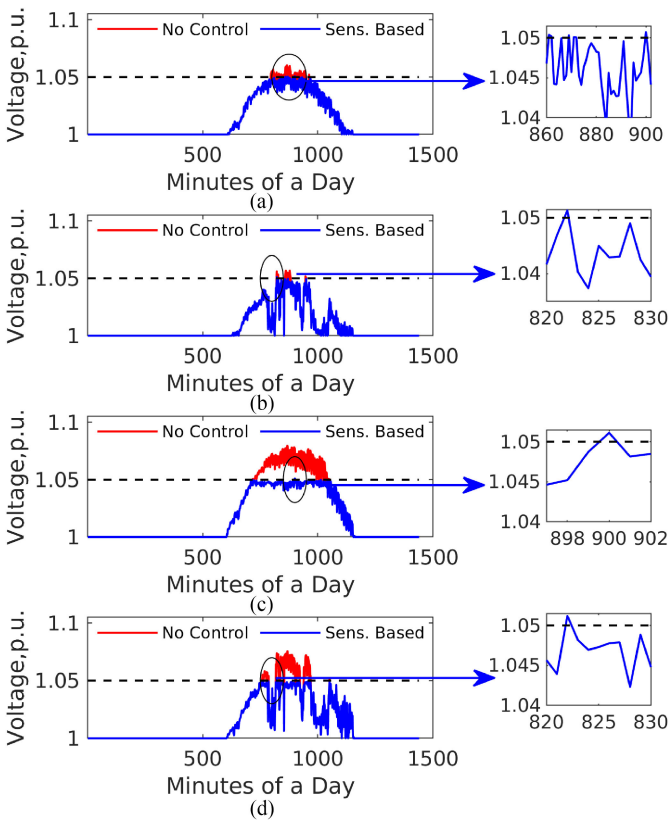

Fig. 11. Max. voltage with base case versus sensitivity-based method. (a) 70% PV, PV-1. (b) 70% PV, PV-2. (c) 100% PV, PV-1. (d) 100% PV, PV-2.

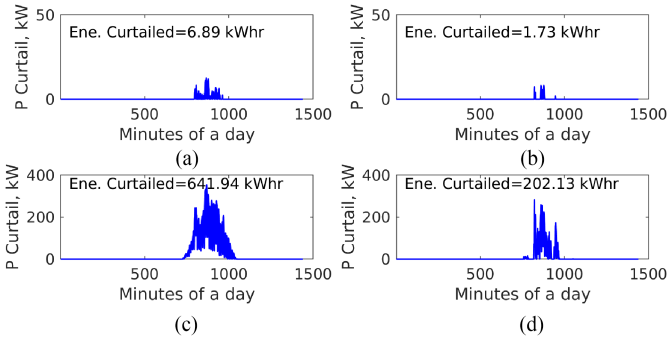

Fig. 12. APC from sensitivity-based method. (a) 70% PV, PV-1. (b) 70% PV, PV-2. (c) 100% PV, PV-1. (d) 100% PV, PV-2.

that the feeder has overvoltage issues during day time when PV output is high.

With droop settings as per the IEEE-1547 guidelines, though the settings are randomized for each inverter, no overvoltage issues were observed. However, it can be seen that the maximum voltage with inverter control is significantly below the maximum allowed limit of 1.05 p.u., which signifies that the droop settings are overly designed and could have caused higher APC and/or higher reactive power output from the PVs. APC of PVs is illustrated in Fig. 10. Nonzero APC means that the reactive power capability of inverters is not sufficient to mitigate overvoltage issues, thus APC becomes necessary. It can be seen from Fig. 10 that with higher PV penetration, the controller needs to curtail higher power from PVs in order to maintain the feeder voltage profile.

C. *Sensitivity-Based Approach*

The simulation results of sensitivity-based method are plotted together with the base case results in Fig. 11. It can be observed that with sensitivity-based method, overvoltage problems can be generally solved. However, there are very few instances where overvoltage still persists. The overvoltage cases are shown in the insets of Fig. 11, and are very close to upper limit of 1.05 p.u. The overvoltage cases are observed around the time when PV outputs are at their maximum. Since, we assumed that not all node voltage measurements are available at the lateral level controller, the proposed approach can lead to instances of overvoltage. Another reason could be attributed to the constant sensitivity, which is computed offline, and leads to error due to approximation.

We illustrate APC obtained from the sensitivity-based in Fig. 12. Compared to the IEEE-1547 droop based approach, APC using sensitivity-based method is less for 70% PV penetration level and more for 100% PV penetration level. As the penetration level increases, more power/energy needs to be curtailed.

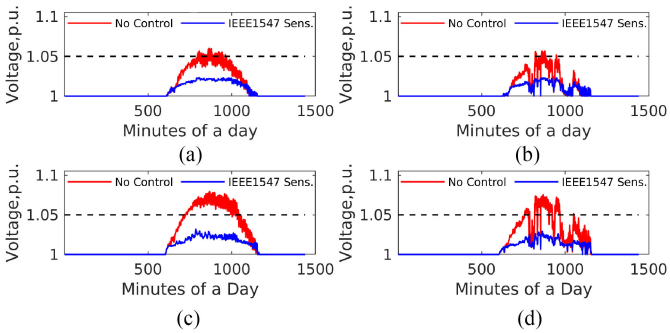

Fig. 13. Max. voltage with base case versus IEEE-1547 droops obtained from the sensitivities. (a) 70% PV, PV-1. (b) 70% PV, PV-2. (c) 100% PV, PV-1. (d) 100% PV, PV-2.

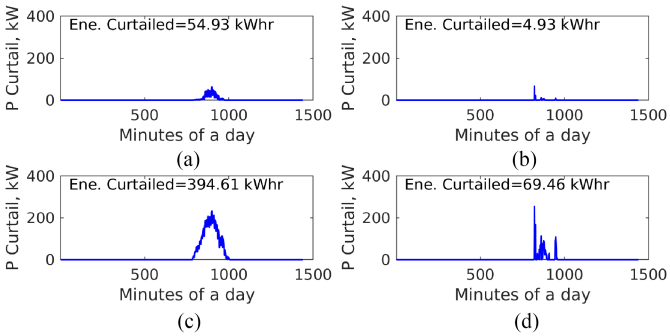

Fig. 14. APC from IEEE-1547 droops obtained from the sensitivities. (a) 70% PV, PV-1. (b) 70% PV, PV-2. (c) 100% PV, PV-1. (d) 100% PV, PV-2.

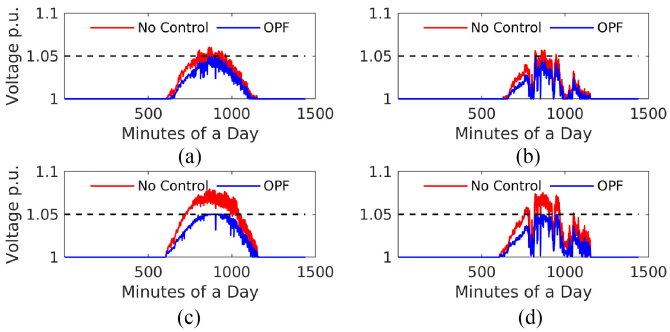

Fig. 15. Max. voltage with base case versus. OPF-based method. (a) 70% PV, PV-1. (b) 70% PV, PV-2. (c) 100% PV, PV-1. (d) 100% PV, PV-2.

D. IEEE-1547 With Power Flow Sensitivities

Simulation results of IEEE-1547-based method using sensitivities are illustrated together with base case results in Fig. 13. It is observed that using sensitivity-based $\boldsymbol{Q(V)}$ droops perform very similar to arbitrarily chosen droops as per the IEEE-1547 (as discussed in Section II-B). Fig. 14 shows APC obtained from the droop settings based on power flow sensitivities.

E. OPF-Based Approach

The maximum feeder voltage profile obtained using OPF-based method is compared with the base case in Fig. 15. From the case studies, it can be seen that the OPF-based approach can completely eliminate the overvoltage issues. APC obtained from OPF-based method is shown in Fig. 16.

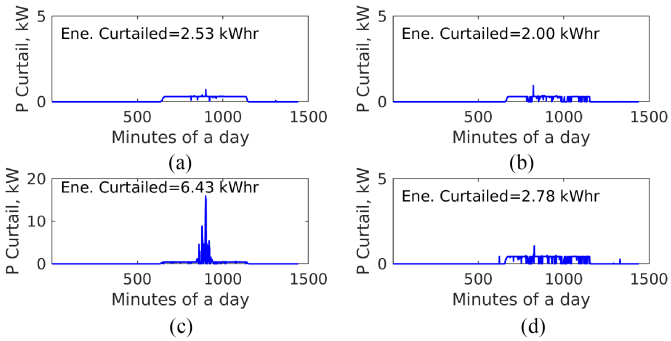

Fig. 16. APC from OPF-based method. (a) 70% PV, PV-1. (b) 70% PV, PV-2. (c) 100% PV, PV-1. (d) 100% PV, PV-2.

TABLE I
COMPARISON OF VPI FOR THE VARIOUS METHODS

PV Profile	PV-1		PV-2	
PV Level	70%	100%	70%	100%
Base Case	0.35	5.22	0.09	2.02
IEEE-1547 Arb.	-2.41	-7.61	-0.65	-3.91
Sensitivity-based	-0.38	-1.09	-0.13	-0.50
IEEE-1547 Sens.	-2.71	-8.49	-0.73	-4.28
OPF-based	-0.54	-1.59	-0.25	-1.28

F. Comparative Analysis

To compare performances of all the methods, we define a voltage performance index (VPI) based on voltage profile compared to maximum allowed upper bound of 1.05 p.u. Let us consider $\boldsymbol{\omega}$ represents the window of time in which over-voltage occurred for the base case simulation. Then, VPI for each method and PV penetration scenario is obtained as: VPI $= \sum_{j,t\in\boldsymbol{\omega}} (\boldsymbol{V}_{j,t} - 1.05)$. A lower value of VPI is desired and a value of zero means a perfect voltage performance. Since the main objective of the controllers would be to keep the voltage below 1.05 p.u., a voltage profile significantly below 1.05 p.u. may suggest unnecessary use of reactive power or APC of PVs. Therefore, an ideal control method would try to keep the voltage just below 1.05 p.u. but as close to 1.05 p.u. as possible. Table I shows summary of VPI in p.u. The base case shows positive VPI, which means the overvoltage issue exists on the feeder. From the results, it can be observed that the sensitivity-based method yields minimum VPI even though the sensitivity-based approach may not completely mitigate the overvoltage issue. It is interesting to note that the VPI for sensitivity-based method is even better than the OPF-based method, and this could possibly because of local optimal solutions of OPF-based approach given the OPF model is nonconvex in nature. The droop settings (as per the IEEE-1547), whether that be arbitrary slopes or slopes based on sensitivity-based approach, yield large negative VPI values. This means these methods unnecessarily over corrects

TABLE II
COMPARISON OF ENERGY CURTAILMENT FOR THE VARIOUS METHODS (IN THE MULTIPLES OF ENERGY CURTAILMENT OBTAINED FROM OPF)

PV Profile	PV-1		PV-2	
PV Level	70%	100%	70%	100%
IEEE-1547 Arb.	14.64	54.27	1.95	24.53
Sensitivity-based	2.72	99.83	0.87	72.71
IEEE-1547 Sens.	21.72	61.37	2.47	24.99

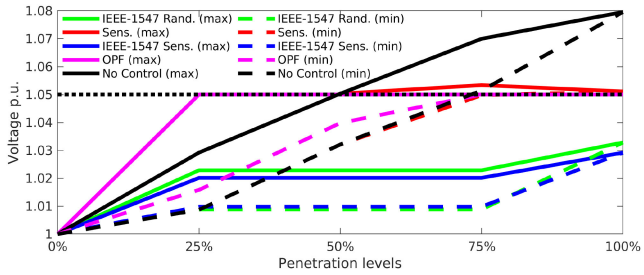

Fig. 17. Voltage performance obtained from Monte Carlo simulation by varying PV penetration level.

the overvoltage issue as the voltage profile is significantly below 1.05 p.u. (see Figs. 9 and 13).The comparison of energy curtailment obtained from all methods with respect to OPF-based (in the multiples of energy curtailment obtained from OPF) is given in Table II. The energy curtailment of OPF-based method is generally minimum. However, there could be cases when the OPF solution is local optimal and, hence, the energy curtailment obtained from OPF may become larger than other methods (see sensitivity-based method for 70% PV penetration with the second PV profile). Energy curtailments obtained from both IEEE-1547 droop-based methods are similar. Though the VPI of sensitivity-based method is better, the sensitivity-based method often leads to larger power/energy curtailments compared to the IEEE-1547 droop-based methods.

G. Monte Carlo Simulation

We also performed Monte Carlo simulation by varying PV penetration level to evaluate the average performance of the four approaches. For each penetration level (randomized 25%, 50%, 75%, and 100% by varying PV location), 1000 different simulations were run for base case, IEEE-1547 with arbitrary settings, sensitivity-based method, IEEE-1547 with sensitivity-based settings, and OPF-based method. The minimum and maximum of the maximum feeder voltage obtained from the 1000 runs are shown in Fig. 17 along with the upper voltage bound of 1.05 p.u. The feeder exhibits overvoltage issues above 50% penetration level without any control. IEEE-1547 overvoltage with arbitrary settings, IEEE-1547 with sensitivity-based settings, and OPF-based approaches are able to solve overvoltage issue for any penetration level. On the other hand, sensitivity-based method may not mitigate overvoltage issue completely as slight overvoltage above 1.05 p.u are observed occasionally.

IV. CONCLUSION

This work developed methods to locally control active/reactive power of smart inverters to regulate voltage profile on distribution feeders. First, a nodal sensitivity-based approach is adopted, and then combined with $Q(V)$ droops as per the IEEE-1547 standard. Then, the performance is compared with arbitrary $Q(V)$ droop settings and an OPF-based approach using a 730-node MV/LV with hundreds of PV inverters. The case studies demonstrate that the droop settings as per the IEEE-1547 can effectively mitigate overvoltage issues. However, the droop settings tend to be overly designed that cause unnecessarily higher correction of overvoltage issues as the resulting voltage profiles become significantly below the allowed voltage upper bounds. A sensitivity-based approach, though not fully able to solve the overvoltage problems, provides the best VPI to mitigate the overvoltage issues by lowering the overvoltage magnitudes in the close vicinity of upper bounds. Given the communication need for centralized OPF-based method and despite nonoptimal APC, the local droop-based approaches could still be alternatives to regulate voltage on distribution feeders with high penetration of PVs. As the penetration of smart inverter increases, and communication infrastructure becomes readily available, a centralized OPF-based control scheme could also become viable.

REFERENCES

[1] F. Katiraei and J. R. Aguero, "Solar PV integration challenges," *IEEE Power Energy Mag.*, vol. 9, no. 3, pp. 62–71, May 2011.
[2] Y. Liu, J. Bebic, B. Kroposki, J. de Bedout, and W. Ren, "Distribution system voltage performance analysis for high-penetration PV," in *Proc. IEEE Energy 2030 Conf.*, Nov. 2008, pp. 1–8.
[3] A. Chidurala, T. K. Saha, and N. Mithulananthan, "Harmonic impact of high penetration photovoltaic system on unbalanced distribution networks-learning from an urban photovoltaic network," *IET Renewable Power Gener.*, vol. 10, no. 4, pp. 485–494, 2016.
[4] R. Tonkoski, L. A. Lopes, and T. H. El-Fouly, "Coordinated active power curtailment of grid connected PV inverters for overvoltage prevention," *IEEE Trans. Sustain. Energy*, vol. 2, no. 2, pp. 139–147, Apr. 2011.
[5] Y. Ueda, K. Kurokawa, T. Tanabe, K. Kitamura, and H. Sugihara, "Analysis results of output power loss due to the grid voltage rise in grid-connected photovoltaic power generation systems," *IEEE Trans. Ind. Electron.*, vol. 55, no. 7, pp. 2744–2751, Jul. 2008.
[6] D. McPhail, B. Croker, and B. Harvey, "A study of solar PV saturation limits for representative low voltage networks," in *Proc. Australas. Univ. Power Eng. Conf.*, 2016, pp. 1–6.
[7] I. Roytelman, B. K. Wee, and R. L. Lugtu, "Volt/var control algorithm for modern distribution management system," *IEEE Trans. Power Syst.*, vol. 10, no. 3, pp. 1454–1460, Aug. 1995.
[8] S. R. Abate, T. E. McDermott, M. Rylander, and J. Smith, "Smart inverter settings for improving distribution feeder performance," in *Proc. IEEE Power Energy Soc. General Meeting*, 2015, pp. 1–5.
[9] F. Ding *et al.*, "Photovoltaic impact assessment of smart inverter volt-VAR control on distribution system conservation voltage reduction and power quality," Nat. Renewable Energy Lab., Golden, CO, USA, Tech. Rep. NREL/TP-5D00-67296, 2016.
[10] *IEEE Standard for Interconnection and Interoperability of Distributed Energy Resources With Associated Electric Power Systems Interfaces, IEEE Standard 1547-2018* (Revision of IEEE Standard 1547-2003), 2018, pp. 1–138.
[11] S. Paudyal, B. P. Bhattarai, R. Tonkoski, S. Dahal, and O. Ceylan, "Comparative study of active power curtailment methods of PVs for preventing overvoltage on distribution feeders," in *Proc. IEEE Power Energy Soc. General Meeting*, 2018, pp. 1–5.
[12] C.-H. Lin, W.-L. Hsieh, C.-S. Chen, C.-T. Hsu, and T.-T. Ku, "Optimization of photovoltaic penetration in distribution systems considering annual duration curve of solar irradiation," *IEEE Trans. Power Syst.*, vol. 27, no. 2, pp. 1090–1097, May 2012.

[13] S. Ghosh, S. Rahman, and M. Pipattanasomporn, "Distribution voltage regulation through active power curtailment with PV inverters and solar generation forecasts," *IEEE Trans. Sustain. Energy*, vol. 8, no. 1, pp. 13–22, Jan. 2017.

[14] A. Molina-García *et al.*, "Reactive power flow control for PV inverters voltage support in LV distribution networks," *IEEE Trans. Smart Grid*, vol. 8, no. 1, pp. 447–456, Jan. 2017.

[15] G. Mokhtari, A. Ghosh, G. Nourbakhsh, and G. Ledwich, "Smart robust resources control in LV network to deal with voltage rise issue," *IEEE Trans. Sustain. Energy*, vol. 4, no. 4, pp. 1043–1050, Oct. 2013.

[16] O. Gagrica, P. H. Nguyen, W. L. Kling, and T. Uhl, "Microinverter curtailment strategy for increasing photovoltaic penetration in low-voltage networks," *IEEE Trans. Sustain. Energy*, vol. 6, no. 2, pp. 369–379, Apr. 2015.

[17] T. T. Ku, C. H. Lin, C. S. Chen, C. T. Hsu, W. L. Hsieh, and S. C. Hsieh, "Coordination of PV inverters to mitigate voltage violation for load transfer between distribution feeders with high penetration of PV installation," *IEEE Trans. Ind. Appl.*, vol. 52, no. 2, pp. 1167–1174, Mar. 2016.

[18] E. Demirok *et al.*, "Local reactive power control methods for overvoltage prevention of distributed solar inverters in low-voltage grids," *IEEE J. Photovolt.*, vol. 1, no. 2, pp. 174–182, Oct. 2011.

[19] M. E. Baran and I. M. El-Markabi, "A multiagent-based dispatching scheme for distributed generators for voltage support on distribution feeders," *IEEE Trans. Power Syst.*, vol. 22, no. 1, pp. 52–59, Feb. 2007.

[20] S. Weckx, C. Gonzalez, and J. Driesen, "Combined central and local active and reactive power control of PV inverters," *IEEE Trans. Sustain. Energy*, vol. 5, no. 3, pp. 776–784, Jul. 2014.

[21] X. Su, M. A. Masoum, and P. J. Wolfs, "Optimal PV inverter reactive power control and real power curtailment to improve performance of unbalanced four-wire LV distribution networks," *IEEE Trans. Sustain. Energy*, vol. 5, no. 3, pp. 967–977, Jul. 2014.

[22] J. Zhao *et al.*, "Optimal and fair real power capping method for voltage regulation in distribution networks with high PV penetration," in *Proc. IEEE Power Energy Soc. General Meeting*, Jul. 2015, pp. 1–5.

[23] G. Cavraro, S. Bolognani, R. Carli, and S. Zampieri, "The value of communication in the voltage regulation problem," in *Proc. IEEE 55th Conf. Decis. Control*, Dec. 2016, pp. 5781–5786.

[24] P. Jahangiri and D. C. Aliprantis, "Distributed Volt/VAr control by PV inverters," *IEEE Trans. Power Syst.*, vol. 28, no. 3, pp. 3429–3439, Aug. 2013.

[25] P. D. F. Ferreira, P. M. S. Carvalho, L. A. F. M. Ferreira, and M. D. Ilic, "Distributed energy resources integration challenges in low-voltage networks: Voltage control limitations and risk of cascading," *IEEE Trans. Sustain. Energy*, vol. 4, no. 1, pp. 82–88, Jan. 2013.

[26] F. Olivier, P. Aristidou, D. Ernst, and T. V. Cutsem, "Active management of low-voltage networks for mitigating overvoltages due to photovoltaic units," *IEEE Trans. Smart Grid*, vol. 7, no. 2, pp. 926–936, Mar. 2016.

[27] M. E. Baran and F. F. Wu, "Network reconfiguration in distribution systems for loss reduction and load balancing," *IEEE Trans. Power Del.*, vol. 4, no. 2, pp. 1401–1407, Apr. 1989.

[28] H. K. Vemprala, M. A. I. Khan, and S. Paudyal, "Open-source poly-phase distribution system power flow analysis tool (DxFlow)," in *Proc. IEEE Int. Conf. Electro Inf. Technol.*, 2019, pp. 1–6.